The Eurasia Proceedings of Science, Technology, Engineering & Mathematics (EPSTEM)
ISSN: 2602-3199

The Eurasia Proceedings of Science, Technology, Engineering & Mathematics (EPSTEM), 2023

Volume 23, Pages 117-123

ICRETS 2023: International Conference on Research in Engineering, Technology and Science

Microstructure and Mechanical Properties Analysis of Al-6061/B4C Composites Fabricated by Conventional and Bobbin Tool Friction Stir Processing

Dhaivat Divekar
Pandit Deendayal Energy University

Kishan Fuse
Pandit Deendayal Energy University

Vishvesh Badheka
Pandit Deendayal Energy University

Abstract: Friction stir processing (FSP) is one of the solid-state processing technique that has gained significant attention from researchers and engineers for fabricating composites. Bobbin tool friction stir processing (BTFSP) is a novel version of conventional FSP. In the present paper, 6 mm thick plates of Al-Mg-Si (6061Al –T6) were subjected to BTFSP and CFSP using B_4C reinforcement particles for comparison. The reinforcement particle distribution and mechanical properties were investigated in the fabricated composites. Agglomeration was observed in BTFSP composites. The crack formation in the BTFSP was due to the absence of forging action, which deposited the B_4C particles in the crack. CFSP composites obtained uniform distribution of the B_4C particles at the top surface. The tilt of the tool in CFSP helped in effective forging action by the shoulder at the trailing edge. Micro-hardness results indicated improved hardness at the top surface for both the processed composites.

Keywords: Friction stir processing, Bobbin tool, Composite, Tilt angle, Microhardness

Introduction

Space applications and automobile industries find aluminium the best choice. The light weight of the parts manufactured from aluminium gives the industries a technical and cost-effective solution (Patidar & Rana, 2017). It has outstanding strength and possesses excellent electrical and thermal properties. Composite materials are replacing conventional materials in industries because of their unmatched elastic modulus, high strength, incredible resistance to fatigue, creep, wear, corrosion, etc. (Jaiswal et al., 2022). Various processes can employ composite fabrication. Some popular techniques to enhance the surface finish are high-energy electron transfer (Kumar et al., 2020), Laser-based surface modification (Quazi et al., 2015), Mechanical alloying (Banhart, 2001), Powder metallurgy (Bains et al., 2016), etc. One such process gaining popularity is Friction Stir Processing (FSP). The fabrication of composite using FSP requires depositing reinforcement particles in the desired region. The rotating FSP tool stirs the metal matrix in the processing region and produces a localized composite structure. The FSP technique has emerged from the Friction Stir Welding (FSW) fundamentals. A unique feature of the FSP is its eco-friendly nature. This makes it the most suitable composite fabrication technique for industries (Teo et al., 2021). The fabrication of the composite using FSP is done significantly through plasisazing of the material, material stirring and mixing, and thermal exposure. Moreover, the FSP leads to homogenous distribution and improved density of the reinforced material in the processed region (Ma, 2008).

- This is an Open Access article distributed under the terms of the Creative Commons Attribution-Noncommercial 4.0 Unported License, permitting all non-commercial use, distribution, and reproduction in any medium, provided the original work is properly cited.
- Selection and peer-review under responsibility of the Organizing Committee of the Conference
© 2023 Published by ISRES Publishing: www.isres.org

Conventional FSP technique has been explored to a great extent in fabricating composites. The size of the grains escalated as there was an increment in the rotation of the tool speed between 300 to 700 rpm during FSP on Al 6063. With incrementing speed, the strength raised slowly and then became more than the BM. Eventually, strain results were all below than BM (Zhao et al., 2019). Hybrid FSP with simultaneous cooling approach enhanced superplastic behavior. Various cooling rates were achieved by introducing varied cooling mediums, such as water and gaseous mediums like compressed air and carbon dioxide , during FSP on AA 7075 alloy (Patel et al., 2019). Al6082 metal matrix was fabricated in composite by adding $CaCO_3$ particles using FSP to study friction and wear properties. Adding $CaCO_3$ doubled the wear properties of FSPed Al6082/$CaCO_3$ composite compared to the FSPed Al6082 (Sivanesh Prabhu et al., 2019).

The rotational speed did not affect much on the tensile strength of the metal. It was recommanded that the multiple passes led to a detoration in the strength of the metal. The feed rate has positive corelation to the UTS of the composite created. Dynamic recrystallization of the grains was seen with as the passes increased.(El-Rayes & El-Danaf, 2012). The Al 6061-T6 sheet fabricated using FSP with TiB2 as the reinforcement material was subjected to a pin-on-disc wear resistance test at a higher temperature. The results showed that the increase in the reinforcement in the composite reduced strength (Rao & Mallikarjuna Rao, 2018). Al-6061 sheets which were 3 mm thick were examined using stationary-shoulder FSP (SFSP) and CFSP. All the process parameters were kept similar for both composites. For a defect-free composite, the CFSP composite showed a better tensile strength, and the SFSP had a tensile strength lower than 10% compared to the CFSP. However, the SFSP composite showed better elongation than the CFSP since the SFSP had fine microstructures at the fracture location (Chen et al., 2020). 3 mm deep composite surface was fabricated in aluminium 6061-T651 alloy plate by reinforcing with sub-micro-size Al_2O_3 and SiC particles. This processed composite showed a reduced friction and wear by 40% and 90% respectively compared to the base metal. Further enhancement was noted in the plate after post-FSP heat treatment. The incremented dislocation density in the composite surface is a possible reason for such enhanced properties in the metal composite (Qu et al., 2011). A aluminium sheet was prepared using WAAM, and post WAAM a, FSP was done on the plate. The FSP helped enhance the microstructure and contributed towards porosity reduction. For instance, a significant drop in the grain size was observed (it reduced from128 μm to 5 μm). The decreased porosity and enhanced microstructure enable microhardness, yield strength, and ultimate tensile strength to increase by 31.5 %, 23.3 %, and 6.0 %, respectively (He et al., 2023). A variation in the FSPed composites was observed with the variation of the eccentricity of the tool's pin. The experimentation showed that the Pin Affected Zone (PAZ) enlarged, and size of the grain in the stir zone was reduced with an increment in the eccentricity of the tool pin. The composite produced with a pin without eccentricity showed higher hardness and yield strength than the one created with pin eccentricity. However, the FSPed composite with an eccentric pin showed an overall escalation in the tensile properties in FSP composite (Chen et al., 2019). A 12 mm thick aluminium alloy (Al-6061-T6) was subjected to general FSP. The experimentation revealed that there was a five times increment in the impact toughness and very good tensile property was exhibited. A detailed study revealed that, the second phase had even distribution of particles. Such enhancement in the properties are reasoned to homogenised deformation, evolved recrystallized microstructure, refined grains, and quality of SZ, moreover the homogeneous distribution of the precipitates adds to this property enhancement. When it comes to the processing of aluminium and B_4C via FSP, the main parameters that affect the results are the speed of the tool rotation, speed of traverse, and the tool tilt angle (Rathee et al., 2016).

Bobbin tool friction stir processing (BTFSP) is one of the novel variants of CFSP. BTFSP is based on a similar principle to CFSP. The BTFSP tool consists of a double shoulder arrangement compared to the CFSP tool (Cui et al., 2009). This modification in the tool delivers many advantages over CFSP, such as dual-side composite fabrication, easy set-up requirement, improved stirring, the requirement of the less rigid machine, etc. Although BTFSP has the potential to eliminate many limitations of FSW/FSP, it has been less explored by researchers (Fuse & Badheka, 2019). Aluminium sheet (Al-6061 T6) of 6 mm thickness was introduced to a bobbin tool FSP for dual-sided composite preparation with B_4C as the reinforcement. Very precise and uniform distribution of the B_4C particles was observed on the lower side of the composite. Experimentation results were enhanced when the number of passes was increased to three. The grain refinement and the even distribution of the reinforcement particles helped to achieve better microhardness as well as wear properties of the composite that was fabricated (Fuse et al., 2021). The comparative studies between BTFSW and CFSW have revealed that the BTFSW show equivalent or slightly higher strength values than the CFSW (Yang et al., 2018). Moreover, some studies even admitted that the process parameters' combined effect helped the BTFSW joints compared with CFSW and helped the BTFSWed joints gain higher strength (Esmaily et al., 2016). The authors of this paper compared the composites fabricated using conventional FSP and Bobbin tool FSP with B_4C reinforcement. This research has been carried out using B_4C (Boron Carbide) as the reinforcement material because the high hardness and low density of B4C make it a perfect fit for defense applications (Patidar & Rana, 2017).

Experimental Methodology

The base plates for the CFSP and BTFSP were cut in the required dimension of 150 x 100 x 6 mm in aluminium 6061-T6 plate. The plates were then prepared for packing the B4C powder by making a grove of 1.5 mm depth and 2 mm wide. A wire cut EDM machine was used to prepare the groove with high precision in both the aluminium plates. The B4C reinforcement particles are mixed in an acetone solution. Further, the mixture was filled in the grooved composite. The plates were kept to dry and let the acetone evaporate, eventually filling the grove with B4C powder.

Figure 1. Vertical milling machine used for experiments

The fabrication of compoistes was done on a vertically oriented semi-automatic milling machine, as shown in Figure 1. A pinless tool was used to cover the grove so that the B4C powder does not escape due to vibration while processing. The bobbin tool used for the BTFSP had symmetric upper and lower shoulders connected via a pin with three flats. The tool's Shoulder diameter and the diameter and height of the pin were 22 mm, 8 mm, and 6 mm, respectively. The tool used for CFSP had a single shoulder of 22 mm diameter and a tapered pin. The tools used during experiments are presented in Figure 2. A rotational speed of 1500 rpm was maintained for both experiments. The machine's feed rate was set constant at 33 mm/min. The angle of tilt for the tool was 2o for CFSP and 0o for BTFSP processes. Three passes were made for BTFSP and CFSP. The fabricated composite composites were further grinded, polished, and then etched using Keller's reagent (NHO3: HCl: HF: H2O = 2.5: 1.5: 1: 95 vol%) to reveal the grain structure of the processed region. The microstructural observations were carried out using Olympus upright metallurgical microscope with a range of 50X- 2000X. The hardness was measured at an interval of 1 mm along the longitudinal direction. The hardness measurement was carried out along the top and middle (2 mm and 4 mm from the upper surface, respectively) on the cross-section which was along the center line. During measurement the load was fixed at 300g for a time span of 10 seconds.

Results and Discussion

Microstructure Analysis of BFSP and CFSP

The optical micrograph of Al 6061-T6 alloy and SEM micrograph of B_4C reinforcement particle is shown in Figure 3. The figure revealed elongated grains of BM.

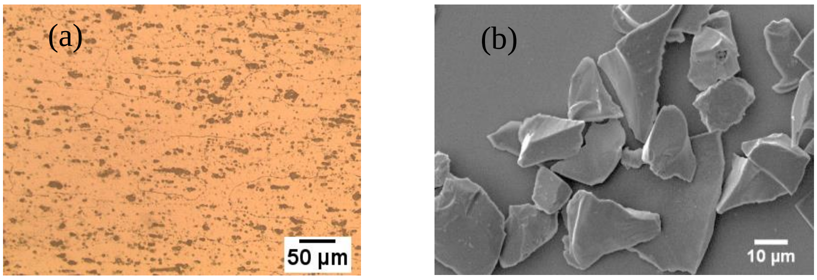

Figure 3. (a) Optical micrograph of Al 6061-T6 aluminium alloy (b) SEM micrograph of B_4C particles

Figure 4 (a) depicts the macrograph of the BTFSPed composite. It indicates the flash formation at the top and bottom of the composite. The both-side flash formation was due to the dual-side shoulder nature of the BTFSP tool, and it suggests the proper grabbing of the aluminium plate. A systematic pattern of alternate lines is visible at the advancing side (AS) of the BTFSPed composite (Figure 4 (b)). The alternate line formation is due to the stirring effect created by the three-face pin that connects the two shoulders of the BTFSP tool. These lines indicate the flow of material and B_4C particles at the AS from the top to the middle of the composite. The shining particles are the B_4C reinforcement particles. It is evident from Figure 4 (b) that the reinforcement material's proper distribution has occurred on the AS of the BTFSPed composite. The macroscopic view of region B in Figure 4 (a) revealed a crack. The magnified view of the crack is presented in Figure 4(c), indicating the agglomeration of the B_4C particles at that region. Figure 4(d) is a microscopic image of region C which is the bottom region of the composite. There is no evidence of any B_4C particle in this region. This is because the B4C particles were deposited up to 1.5 mm depth only. Figure 4 (e) is a magnified view of region D in Figure 4(a). A similar trend of accumulation of the reinforcement particles is seen in this region. Figure 4(f) is a magnified image of region D' in Figure 4(e), which indicate well distributed B_4C particles in the crack. This observation highlights that even though the BTFSP tool had an extra shoulder at the bottom, this lower shoulder has not contributed to spreading B4C particles.

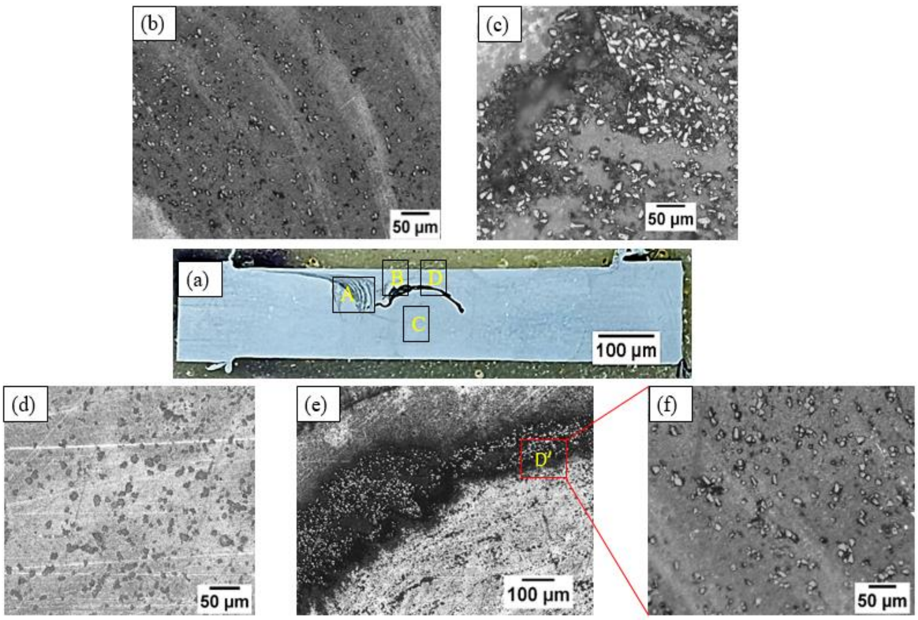

Figure 4. (a) macrostructure image of the BTFSP, (b) magnified image of the region marked as A in (a), (c) magnified image of the region marked as B in (a), (d) magnified image of the region marked as C in (a), (e) magnified image of the region marked as D in (a), (f) magnified image of the region marked as D’ in (e).

Figure 5(a) shows the macroscopic view of the CFSPed composite, which appears to have a U-shaped profile in the SZ. A minor porosity at the top of the SZ on AS can be seen in the macroscopic image. This porosity could be a result of the improper intermixing of B4C particles with plasticized BM. Additionally, It can be noted that the density of B4C particles in the crack zone of the BTFSP composite was much higher than CFSP. The interface of BM and SZ can be easily observed in Figure 5 (b).

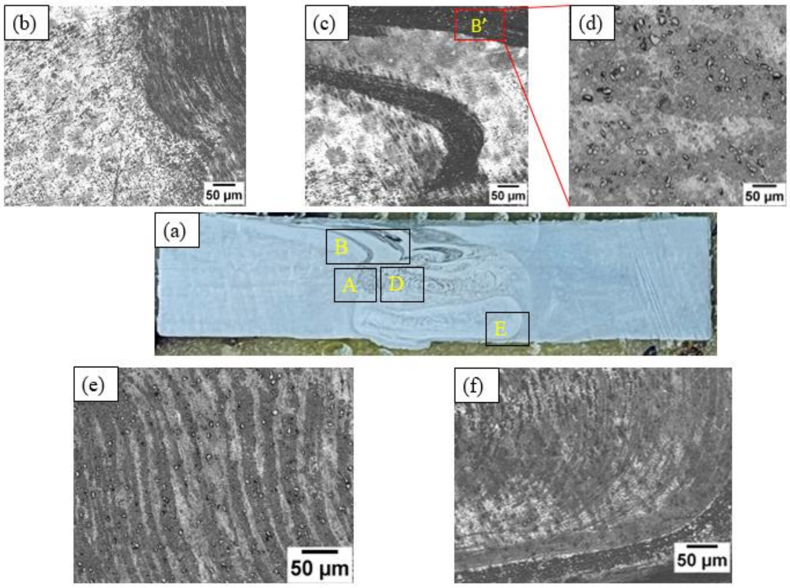

Figure 5. (a) macrostructure image of the CFSP, (b) magnified image of the region marked as A in (a), (c) magnified image of the region marked as B in (a), (d) magnified image of the region marked as B' in (c), (e) magnified image of the region marked as D in (a), (f) magnified image of the region marked as E in (e).

Figure 5(c) shows the magnified view of region B. It is interesting to observe an alternate pattern in the image. This may be due to the threaded pin used in CFSP. This pattern is similar to the BTFSPed composite. But, the distance between the dark strands in the CFSP composite is more significant as compared to the BTFSP. Figure 5 (d) shows the magnified image of region B'. This image reveals a proper and even distribution of the reinforcement particles in the upper region of the SZ. Figure 5(e) shows the microscopic structure of the D region. Flow lines are clearly evident in this zone, and moderate distribution of B_4C particles can also be observed. It is interesting to observe the reinforcement particles in this region, which is the bottom part of the composite. The presence of B4C particles at the bottom can be due to threaded pin because threads tend to move material from top to bottom. Figure 5 (f) shows the bottom region E on the retreating side (RS). The downward marks in the figure revealed the flow of material from the middle to the bottom of the center of SZ on RS.

Microhardness Distribution

Figure 6 shows the graph of the microhardness recorded at different locations and regions of the BTFSP and CFSP composites. The highest recorded hardness value was 85.1 HV for the CFSPed composite in the SZ. It is interesting to observe that the highest value of hardness for BTFSPed was 83.1 HV.

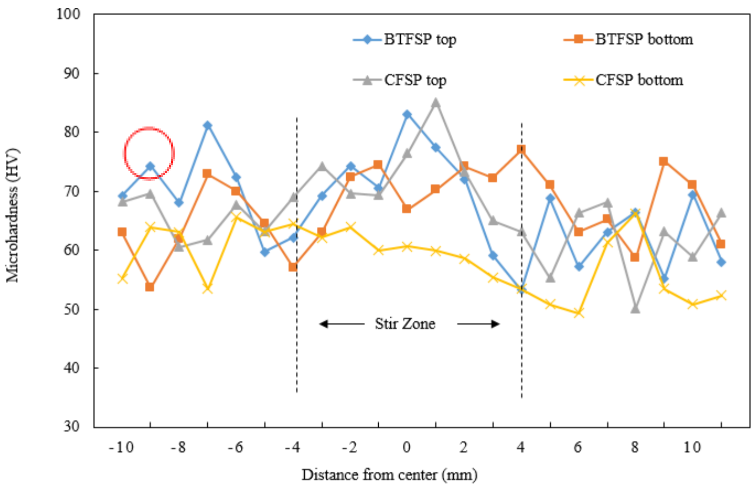

Figure 6. Microhardness distribution in CFSP and BTFSP

The difference in the hardness values of both composites is negligible but can be attributed to proper stirring in the CFSPed composite.It is observed that the average hardness at the top surface of CFSP and BTFSP composites is higher than the bottom surface of both composites. This is obviously due to the presence of B_4C particles at the top surface. The readings of the graph suggest that the average microhardness was 70 HV adjacent to the SZ. The lowest hardness was encountered at the interface of the TMAZ and the HAZ zone. There is an evident spike in the hardness at the top of the BTFSPed composite in the TMAZ with a hardness value of 81.2 HV, as shown by the red circle. This could be due to the striking of an indenter on a B_4C particle at a particular location.

Conclusion

The fabrication of composite of Al 6061/ B_4C was done at the top surface using conventional FSP and a novel bobbin tool technique. The pmicrostructure and microhardness of the developed composites have been exmined. The conclusion of the study can be summarized in the points mentioned below:

1. Microstructural study revealed the agglomerated distribution of the B_4Cparticles in the crack zone in both CFSP and BTFSP composite. However, CFSP composites obtained uniform distribution of the B_4C particles at the top surface.
2. The distance between the dark strands in the CFSP composite is more significant as compared to the BTFSP composite.
3. CFSPed composite exhibited presence of B4C particles in the lower region of the composite due to the threaded pin. No trace of reinforcement particles was found at the bottom for the BTFSPed composite.
4. At the top CFSPed and BTFSPed composites reached maximum microhardness of 85.1 and 83.1 HV, respectively, indicating substantial hardness improvement.

Scientific Ethics Declaration

The authors declare that the scientific ethical and legal responsibility of this article published in EPSTEM journal belongs to the authors.

References

Bains, P. S., Sidhu, S. S., & Payal, H. S. (2016). Fabrication and machining of metal matrix composites: A Review. *Materials and Manufacturing Processes*, *31*(5), 553–573.

Banhart, J. (2001). Manufacture, characterisation and application of cellular metals and metal foams. *Progress in Materials Science*, *46*(6), 559–632.

Chen, Y., Li, H., Wang, X., Ding, H., & Zhang, F. (2020). A comparative study on stationary-shoulder and conventional friction-stir-processed Al-6061 Alloy. *Journal of Materials Engineering and Performance*, *29*(2), 1185–1193.

Chen, Y., Wang, H., Ding, H., Zhao, J., Zhang, F., & Ren, Z. (2019). Effect of tool pin eccentricity on the microstructure and mechanical properties of friction stir processed Al-6061 Alloy. *Journal of Materials Engineering and Performance*, *28*(5), 2845–2852.

Cui, G. R., Ma, Z. Y., & Li, S. X. (2009). The origin of non-uniform microstructure and its effects on the mechanical properties of a friction stir processed Al–Mg alloy. *Acta Materialia*, *57*(19), 5718–5729.

El-Rayes, M. M., & El-Danaf, E. A. (2012). The influence of multi-pass friction stir processing on the microstructural and mechanical properties of Aluminum Alloy 6082. *Journal of Materials Processing Technology*, *212*(5), 1157–1168.

Esmaily, M., Mortazavi, N., Osikowicz, W., Hindsefelt, H., Svensson, J. E., Halvarsson, M., Martin, J., & Johansson, L. G. (2016). Bobbin and conventional friction stir welding of thick extruded AA6005-T6 profiles. *Materials & Design*, *108*, 114–125.

Fuse, K., & Badheka, V. (2019). Bobbin tool friction stir welding: A review. *Science and Technology of Welding and Joining*, *24*(4), 277–304.

Fuse, K., Badheka, V., Patel, V., & Andersson, J. (2021). Dual sided composite formation in Al 6061/B4C using novel bobbin tool friction stir processing. *Journal of Materials Research and Technology*, *13*, 1709–1721.

He, P., Bai, X., & Zhang, H. (2023). Microstructure refinement and mechanical properties enhancement of wire and arc additively manufactured 6061 aluminum alloy using friction stir processing post-treatment. *Materials Letters*, *330*, 133365.

Jaiswal, R., Kumar, A., & Singh, R. (2022). Effect of process parameter on surface composite developed through friction stir processing: A review. In A. Dvivedi, A. Sachdeva, R. Sindhwani, & R. Sahu (Eds.), *Recent Trends in Industrial and Production Engineering* (pp. 1–22). Springer.

Kumar, S., Singh, R., Jaiswal, R., & Kumar, A. (2020). Optimization of process parameters of electron beam welded Fe49Co2V Alloys. *International Journal of Engineering*, *Transactions B: Applications*, *33*, 870–876.

Ma, Z. Y. (2008). Friction stir processing technology: A review. *Metallurgical and Materials Transactions A*, *39*(3), 642–658.

Patel, V., Badheka, V., Li, W., & Akkireddy, S. (2019). Hybrid friction stir processing with active cooling approach to enhance superplastic behavior of AA7075 aluminum alloy. *Archives of Civil and Mechanical Engineering*, *19*(4), 1368–1380.

Patidar, D., & Rana, R. S. (2017). Effect of B4C particle reinforcement on the various properties of aluminium matrix composites: A survey paper. *Materials Today: Proceedings*, *4*(2, Part A), 2981–2988.

Qu, J., Xu, H., Feng, Z., Frederick, D. A., An, L., & Heinrich, H. (2011). Improving the tribological characteristics of aluminum 6061 alloy by surface compositing with sub-micro-size ceramic particles via friction stir processing. *Wear*, *271*(9), 1940–1945.

Quazi, M., M. A., F., Haseeb, A. S. M. A., Yusof, F., Masjuki, H. H., & Ahmed, A. (2015). Laser-based surface modifications of aluminum and its alloys. *Critical Reviews in Solid State and Materials Sciences*, *41*, 1–26.

Rao, Ch. M., & Mallikarjuna Rao, K. (2018). Abrasive wear behaviour of tib2 fabricated aluminum 6061. *Materials Today: Proceedings*, *5*(1, Part 1), 268–275.

Rathee, S., Maheshwari, S., Noor Siddiquee, A., Srivastava, M., & Kumar Sharma, S. (2016). Process parameters optimization for enhanced microhardness of AA 6061/ SiC surface composites fabricated via Friction Stir Processing (FSP). *Materials Today: Proceedings*, *3*(10, Part B), 4151–4156.

Sivanesh Prabhu, M., Elaya Perumal, A., Arulvel, S., & Franklin Issac, R. (2019). Friction and wear measurements of friction stir processed aluminium alloy 6082/CaCO3 composite. *Measurement*, *142*, 10–20.

Teo, G. S., Liew, K. W., & Kok, C. K. (2021). Enhancement of microhardness and tribological properties of recycled AA 6063 using energy-efficient and environment-friendly friction stir processing. *IOP Conference Series: Earth and Environmental Science*, *943*(1), 012019. https://doi.org/10.1088/1755-1315/943/1/012019

Yang, C., Ni, D. R., Xue, P., Xiao, B. L., Wang, W., Wang, K. S., & Ma, Z. Y. (2018). A comparative research on bobbin tool and conventional friction stir welding of Al-Mg-Si alloy plates. *Materials Characterization*, *145*, 20–28.

Zhao, H., Pan, Q., Qin, Q., Wu, Y., & Su, X. (2019). Effect of the processing parameters of friction stir processing on the microstructure and mechanical properties of 6063 aluminum alloy. *Materials Science and Engineering: A*, *751*, 70–79.

Author Information

Dhaivat Divekar
Pandit Deendayal Energy University
Gandhinagar, Gujarat, India-382007
India

Kishan Fuse
Pandit Deendayal Energy University
Gandhinagar, Gujarat, India-382007
India
Contact e-mail: *Kishan.fuse@sot.pdpu.ac.in*

Vishvesh Badheka
Pandit Deendayal Energy University
Gandhinagar, Gujarat, India-382007
India

To cite this article:

Divekar D.N., Fuse K.A., & Badheka V.J. (2023). Microstructure and mechanical properties analysis of Al-6061/B4C composites fabricated by conventional and bobbin tool friction stir processing. *The Eurasia Proceedings of Science, Technology, Engineering & Mathematics (EPSTEM), 23*, 117-123.